PLOS ONE

RESEARCH ARTICLE

Control strategies for COVID-19 epidemic with vaccination, shield immunity and quarantine: A metric temporal logic approach

Zhe Xu[1]*, **Bo Wu**[2], **Ufuk Topcu**[2,3]

1 School for Engineering of Matter, Transport and Energy, Arizona State University, Tempe, AZ, United States of America, **2** Oden Institute for Computational Engineering and Sciences, University of Texas at Austin, Austin, TX, United States of America, **3** Department of Aerospace Engineering and Engineering Mechanics, University of Texas at Austin, Austin, TX, United States of America

* xzhe1@asu.edu

Citation: Xu Z, Wu B, Topcu U (2021) Control strategies for COVID-19 epidemic with vaccination, shield immunity and quarantine: A metric temporal logic approach. PLoS ONE 16(3): e0247660. https://doi.org/10.1371/journal.pone.0247660

Editor: Alessandro Borri, CNR, National Research Council of Italy, ITALY

Received: September 12, 2020

Accepted: February 11, 2021

Published: March 5, 2021

Data Availability Statement: All relevant data are within the paper, and the codes for generating the data are deposited to the GitHub repository (https://github.com/david00710/Covid-19-control).

Funding: This study was funded by the National Science Foundation (https://nsf.gov) in the form of a grant (No. NSF 1652113) awarded to all authors. The funders had no role in study design, data collection and analysis, decision to publish, or preparation of the manuscript.

Competing interests: The authors have declared that no competing interests exist.

Abstract

Ever since the outbreak of the COVID-19 epidemic, various public health control strategies have been proposed and tested against the coronavirus SARS-CoV-2. We study three specific COVID-19 epidemic control models: the susceptible, exposed, infectious, recovered (SEIR) model with vaccination control; the SEIR model with *shield immunity* control; and the susceptible, un-quarantined infected, quarantined infected, confirmed infected (SUQC) model with quarantine control. We express the control requirement in *metric temporal logic* (MTL) formulas (a type of formal specification languages) which can specify the expected control outcomes such as "*the deaths from the infection should never exceed one thousand per day within the next three months*" or "*the population immune from the disease should eventually exceed 200 thousand within the next 100 to 120 days*". We then develop methods for synthesizing control strategies with MTL specifications. To the best of our knowledge, this is the first paper to systematically synthesize control strategies based on the COVID-19 epidemic models with formal specifications. We provide simulation results in three different case studies: vaccination control for the COVID-19 epidemic with model parameters estimated from data in Lombardy, Italy; shield immunity control for the COVID-19 epidemic with model parameters estimated from data in Lombardy, Italy; and quarantine control for the COVID-19 epidemic with model parameters estimated from data in Wuhan, China. The results show that the proposed synthesis approach can generate control inputs such that the time-varying numbers of individuals in each category (e.g., infectious, immune) satisfy the MTL specifications. The results also show that early intervention is essential in mitigating the spread of COVID-19, and more control effort is needed for more *stringent* MTL specifications. For example, based on the model in Lombardy, Italy, achieving less than 100 deaths per day and 10000 total deaths within 100 days requires 441.7% more vaccination control effort than achieving less than 1000 deaths per day and 50000 total deaths within 100 days.

1 Introduction

The COVID-19 pandemic [1] has caused over 28 million confirmed cases and over 0.91 million deaths globally as of September 12, 2020. Ever since the outbreak of COVID-19, various public health control strategies have been proposed and tested against the coronavirus SARS-CoV-2 [2–4].

Currently, over 90 vaccines are being developed against SARS-CoV-2 by research teams across the world [5]. Besides vaccination, other strategies have also been proposed to control the spread of SARS-CoV-2. In [6], the authors proposed *shield immunity* to protect the susceptible people from getting infected with SARS-CoV-2. Specifically, shield immunity works by first identifying and deploying recovered individuals who have protective antibodies to SARS-CoV-2, and then increasing the proportion of interactions with recovered individuals as opposed to other individuals. In [7], the authors analyzed how quarantine has mitigated the spread of SARS-CoV-2 based on a model that differentiates quarantined infected individuals and un-quarantined infected individuals.

Despite the fact that various promising control strategies have been proposed against SARS-CoV-2, such control strategies still suffer from several limitations. (a) The control strategies against SARS-CoV-2 often treat the control inputs (e.g., the shield strength in shield immunity and the quarantine rate in quarantine control) as parameters that stay constant during one stage of time, while in reality such parameters may change on a daily basis with more fine-tuned control. (b) The control inputs in the literature are often tuned manually through trial-and-error instead of being synthesized systematically. (c) There is a lack of specific and formal specifications for the expected effects and outcomes of the control strategies.

To address these limitations, we propose a systematic control synthesis approach for three control strategies against SARS-CoV-2. We use *metric temporal logic* (MTL) formulas to specify the expected control outcomes such as "*the deaths from the infection should never exceed one thousand per day within the next three months*" or "*the population immune from the disease should eventually exceed 200 thousand within the next 100 to 120 days*". Such temporal logic formulas have been used as high-level knowledge or specifications in many applications in artificial intelligence [8], robotic control [9], power systems [10], etc.

The proposed control synthesis approach is based on three specific COVID-19 epidemic mitigation models: the susceptible, exposed, infectious, recovered (SEIR) model with vaccination control; the SEIR model with shield immunity control; and the susceptible, un-quarantined infected, quarantined infected, confirmed infected (SUQC) model with quarantine control. We develop methods for synthesizing control strategies based on the three specific COVID-19 epidemic models with MTL specifications. Specifically, we convert the synthesis problem into mixed-integer bi-linear programming or mixed-integer fractional constrained programming problems, and solve the optimization problems using highly efficient solvers [11].

We provide simulation results in three different case studies: vaccination control for COVID-19 epidemic with model parameters estimated from data in Lombardy, Italy; shield immunity control for COVID-19 epidemic with model parameters estimated from data in Lombardy, Italy; and quarantine control for COVID-19 epidemic with model parameters estimated from data in Wuhan, China. The proposed synthesis approach can generate control inputs such that the time-varying numbers of individuals in each category (e.g., infectious, immune) satisfy the MTL specifications.

Based on the simulation results, we observe that early control is essential in mitigating the spread of COVID-19, and more control effort is needed for more *stringent* MTL specifications. For example, based on the model in Lombardy, Italy, achieving less than 100 deaths per day

and 10000 total deaths within 100 days requires 441.7% more vaccination control effort than achieving less than 1000 deaths per day and 50000 total deaths within 100 days. As the control inputs are generated on a daily basis, the proposed approach can be used to assist and provide quantitative guidelines in public health control strategies to achieve specific specifications for mitigating the spread of COVID-19.

2 Related work

COVID-19 epidemic modeling and control strategies. Ever since the outbreak of COVID-19, there has been numerous research focusing on the modeling of COVID-19 epidemic based on data collected from both the epicenters and other places [12–17]. Among the various models, *compartmental models* such as SEIR and SUQC models have been used frequently for the analysis of COVID-19. There has also been work in analyzing or predicting the spread of COVID-19 using artificial intelligence models [17, 18], stochastic intensity models [13], etc. The models we use in this paper are based on the SEIR (both the standard and with shield immunity) and SUQC models, but we have replaced some essential parameters (e.g., the shield strength in shield immunity, the quarantine rate in quarantine control) with control inputs which can be synthesized to vary on a daily basis.

Optimal control of epidemic models. There exist works in designing vaccination control for the SEIR or SIR models of epidemics [19, 20]. However, such methods have not been applied in the setting of COVID-19. Besides, there has been no work in optimal control of epidemic models with formal specifications (e.g., expressed in temporal logic formulas).

Control synthesis with temporal logic specifications. There are three main categories of approaches to designing controllers that meet temporal logic specifications [21–31]. The first category of approaches abstract the system as a transition system and transform the control syntheses problem into a series of constrained reachability problems [32–34]. The second category of approaches mainly focus on linear dynamical systems and they convert the control synthesis problem into a mixed-integer linear programming (MILP) problem [35–40] which can be solved efficiently by MILP solvers. The third category of approaches substitute the temporal logic constraint into the objective function of the optimization problem and apply a functional gradient descent algorithm on the resulting unconstrained problem [10, 41–43]. The control synthesis approach in this paper is based on the second category of approaches, but we have extended the method to non-linear dynamical systems to fit the epidemic models for COVID-19.

3 Methodology

In this section, we provide the descriptions of methodology for synthesizing control strategies based on the three specific COVID-19 epidemic models with metric temporal logic (MTL) specifications. We first review MTL in Section 3.1, then introduce three control models for COVID-19 epidemic (vaccination control, shield immunity control and quarantine control) in Section 3.2, and finally present the control synthesis methods for the three COVID-19 control models in Section 3.3.

3.1 Metric Temporal Logic (MTL)

In this subsection, we briefly review metric temporal logic (MTL) [44] interpreted over discrete-time trajectories. The state x belongs to the domain $\mathcal{X} \subset \mathbb{R}^n$. The time set is $\mathbb{T} = \mathbb{R}_{\geq 0}$. The domain $\mathbb{B} = \{\text{True}, \text{False}\}$ is the Boolean domain, and the time index set is $\mathbb{I} = \{0, 1, \ldots\}$. We use $t[k] \in \mathbb{T}$ to denote the time instant at time index $k \in \mathbb{I}$ and $x[k] \triangleq x(t[k])$ to denote the value of x at time instant $t[k]$. We use ξ to denote a *trajectory* as a

function from $\mathbb{T}$ to $\mathcal{X}$. A set AP is a set of atomic propositions, each mapping $\mathcal{X}$ to $\mathbb{B}$. For example, the state x can be in the form of $[x_1, x_2]$, where x_1 and x_2 represent the number of deaths from COVID-19 and the number of recovered patients from COVID-19 in a certain geographic region, respectively. Then, an atomic proposition could be in the form of $(x_1 \leq 0.01)$, which means "the number of deaths from COVID-19 in the region does not exceed 0.01 million", or in the form of $(x_2 \geq 6)$, which means "the number of recovered patients from COVID-19 in the region is at least 6 million" (in this paper we assume that the unit in the state is **million**, unless otherwise indicated). In such context, if $x_1 = 0.002$ and $x_2 = 4$, then $(x_1 \leq 0.01)$ is True, and $(x_2 \geq 6)$ is False.

The syntax of MTL is defined recursively as follows:

$$\varphi \coloneqq \top \mid \pi \mid \neg\varphi \mid \varphi_1 \wedge \varphi_2 \mid \varphi_1 \vee \varphi_2 \mid \varphi_1 \mathcal{U}_{\mathcal{I}} \varphi_2, \tag{1}$$

where $\top$ stands for the Boolean constant True, $\pi \in AP$ is an atomic proposition, $\neg$ (negation), $\wedge$ (conjunction), $\vee$ (disjunction) are standard Boolean connectives, $\mathcal{U}$ is a temporal operator representing "until", $\mathcal{I}$ is a time index interval of the form $\mathcal{I} = [i_1, i_2]$ $(i_1 \leq i_2, i_1, i_2 \in \mathbb{I})$. We can also derive two useful temporal operators from "until" $(\mathcal{U})$, which are "eventually" $\Diamond_{\mathcal{I}}\varphi = \top\mathcal{U}_{\mathcal{I}}\varphi$ and "always" $\Box_{\mathcal{I}}\varphi = \neg\Diamond_{\mathcal{I}}\neg\varphi$. Following the example of $x = [x_1, x_2]$, where x_1 and x_2 represent the number of deaths from COVID-19 and the number of recovered patients from COVID-19 in a certain geographic region, respectively, an MTL formula can be in the form of $\Box_{[0,100]}(x_1 \leq 0.01) \wedge \Diamond_{[40,60]}(x_2 \geq 6)$, which means "the number of deaths from COVID-19 should never exceed 0.01 million within the next 100 days, and the number of recovered patients from COVID-19 should be at least 6 million for at least one day within the next 40 to 60 days" (in this paper we assume that the unit in $\mathcal{I}$ is **day** in this paper, unless otherwise indicated).

We define the set of states that satisfy the atomic proposition π as $\mathcal{O}(\pi) \subset \mathcal{X}$. We denote $\langle\langle\varphi\rangle\rangle(\xi, k) = \top$ if the trajectory ξ satisfies the formula φ at discrete-time instant $t[k]$ $(k \in \mathbb{I})$. Then the Boolean semantics of MTL are defined recursively as follows [45]:

$$\begin{aligned}
\langle\langle\top\rangle\rangle(\xi, k) &\coloneqq \top, \\
\langle\langle\pi\rangle\rangle(\xi, k) &\coloneqq x[k] \in \mathcal{O}(\pi), \\
\langle\langle\neg\varphi\rangle\rangle(\xi, k) &\coloneqq \neg\langle\langle\varphi\rangle\rangle(\xi, k), \\
\langle\langle\varphi_1 \vee \varphi_2\rangle\rangle(\xi, k) &\coloneqq \langle\langle\varphi_1\rangle\rangle(\xi, k) \vee \langle\langle\varphi_2\rangle\rangle(\xi, k), \\
\langle\langle\varphi_1 \mathcal{U}_{\mathcal{I}} \varphi_2\rangle\rangle(\xi, k) &\coloneqq \bigvee_{k' \in (k+\mathcal{I})} (\langle\langle\varphi_2\rangle\rangle(\xi, k') \wedge \bigwedge_{k \leq k'' < k'} \langle\langle\varphi_1\rangle\rangle \\
&\quad (\xi, k'')),
\end{aligned} \tag{2}$$

where $k + \mathcal{I} = \{k + \tilde{k} | \tilde{k} \in \mathcal{I}\}$.

3.2 COVID-19 models with control strategies

In this subsection, we study three models for COVID-19 epidemic [6, 7, 14] and introduce the corresponding models with vaccination control, shield immunity control and quarantine control.

COVID-19 SEIR model with vaccination control. The susceptible, exposed, infectious, recovered (SEIR) model has been frequently used in epidemic analyses. As shown in Fig 1, the total population is divided into five subgroups:

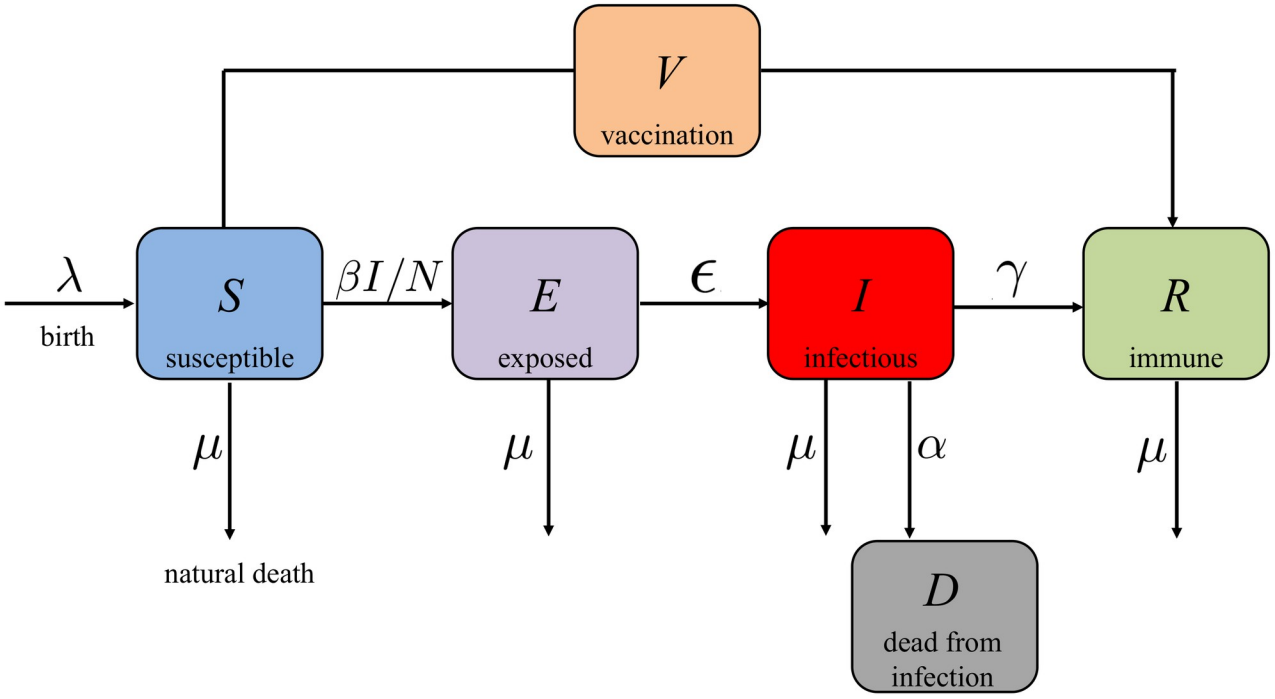

Fig 1. Block diagram of the COVID-19 SEIR model with vaccination control.

https://doi.org/10.1371/journal.pone.0247660.g001

- The susceptible population S: everyone is susceptible to the disease by birth since immunity is not hereditary;
- The exposed population E: the individuals who have been exposed to the disease, but are still not infectious;
- The infectious population I: the individuals who are infectious;
- The immune (recovered) population R: the individuals who are vaccinated or recovered from the disease, i.e., the population who are immune to the disease;
- The dead population D: the dead individuals from the disease.

We consider a COVID-19 SEIR model [14, 15] with vaccination control [19] as follows.

$$\begin{aligned}
\dot{I} &= \epsilon E - (\gamma + \mu + \alpha)I; \\
\dot{E} &= \beta SI/N - (\mu + \epsilon)E; \\
\dot{S} &= \lambda N - \mu S - \beta SI/N - V; \\
\dot{R} &= \gamma I - \mu R + V; \\
\dot{D} &= \alpha I,
\end{aligned} \tag{3}$$

where the control input V is the number of vaccinated individuals per day, $N = S + E + I + R \leq N_0$ is the total population in the region (N_0 is the initial total population in the region), S, E, I, R and D are the number of susceptible, exposed, infectious and recovered population in the

region, respectively, and D is the number of deaths from SARS-CoV-2 in the region. For the parameters, λ denotes the per-capita birth rate, μ is the per-capita natural death rate (death rate from causes unrelated to SARS-CoV-2), α is the SARS-CoV-2 virus-induced average fatality rate, β is the probability of disease transmission per contact (dimensionless) times the number of contacts per unit time, ϵ is the rate of progression from exposed to infectious (the reciprocal is the incubation period), and γ is the recovery rate of infectious individuals (the reciprocal is the infectious period). In this paper, we assume that the birth rate and the natural death rate are the same for the population we are investigating, i.e., $\lambda = \mu$. Hence, from (3) we can derive that $\dot{D} = -\dot{I} - \dot{E} - \dot{S} - \dot{R}$ which means that $I + E + S + R + D$ does not change over time. Therefore, we have $D = N_0 - I - E - S - R = N_0 - N$.

Remark 1. *Note that one difference between this model and the vaccination control model in* [19] *is that we control V as the number of vaccinated individuals per day (constrained to be less than the susceptible population S), while in* [19] *the control input is the ratio of the vaccinated individuals per day to the average born population per day. We found it more convenient this way for computational convenience in the control synthesis in Section 3.3.*

COVID-19 SEIR model with shield immunity control. *Shield immunity* is a strategy recently proposed in [6] to limit the transmission of SARS-CoV-2. The basic idea of this strategy is to increase the proportion of interactions with recovered individuals as opposed to the other individuals in the population. The effectiveness of this strategy is based on the assumption that recovered individuals (virus-negative and antibody-positive) can safely interact with both susceptible and infectious individuals without getting infected with the disease.

As the model used in [6] is modified from an SIR model, we consider a corresponding SEIR model with shield immunity control as follows (see Fig 2 as an illustration).

$$\begin{aligned}
\dot{I} &= \epsilon E - (\gamma + \mu + \alpha) I; \\
\dot{E} &= \beta S I/(N + \chi R) - (\mu + \epsilon) E; \\
\dot{S} &= \lambda N - \mu S - \beta S I/(N + \chi R); \\
\dot{R} &= \gamma I - \mu R; \\
\dot{D} &= \alpha I,
\end{aligned} \tag{4}$$

where the states and parameters are the same as in (3), while $\chi(\cdot)$ is the *shield strength* [6] as control input to be synthesized for the recovered population to substitute the contact for the susceptible population.

COVID-19 SUQC model with quarantine control. The susceptible, un-quarantined infected, quarantined infected, confirmed infected (SUQC) model was recently proposed in [7] based on the COVID-19 data in Wuhan, China. As shown in Fig 3, we consider four subgroups in the population:

- The susceptible population S: everyone is susceptible to the disease by birth since immunity is not hereditary;
- The un-quarantined infected population U: the individuals who are infected and un-quarantined, and they can be either asymptomatic or symptomatic;
- The quarantined infected population Q: the individuals who are infectious and quarantined (the un-quarantined infected become quarantined infected by isolation or hospitalization, and the quarantined infected lose the ability of infecting the susceptible individuals);

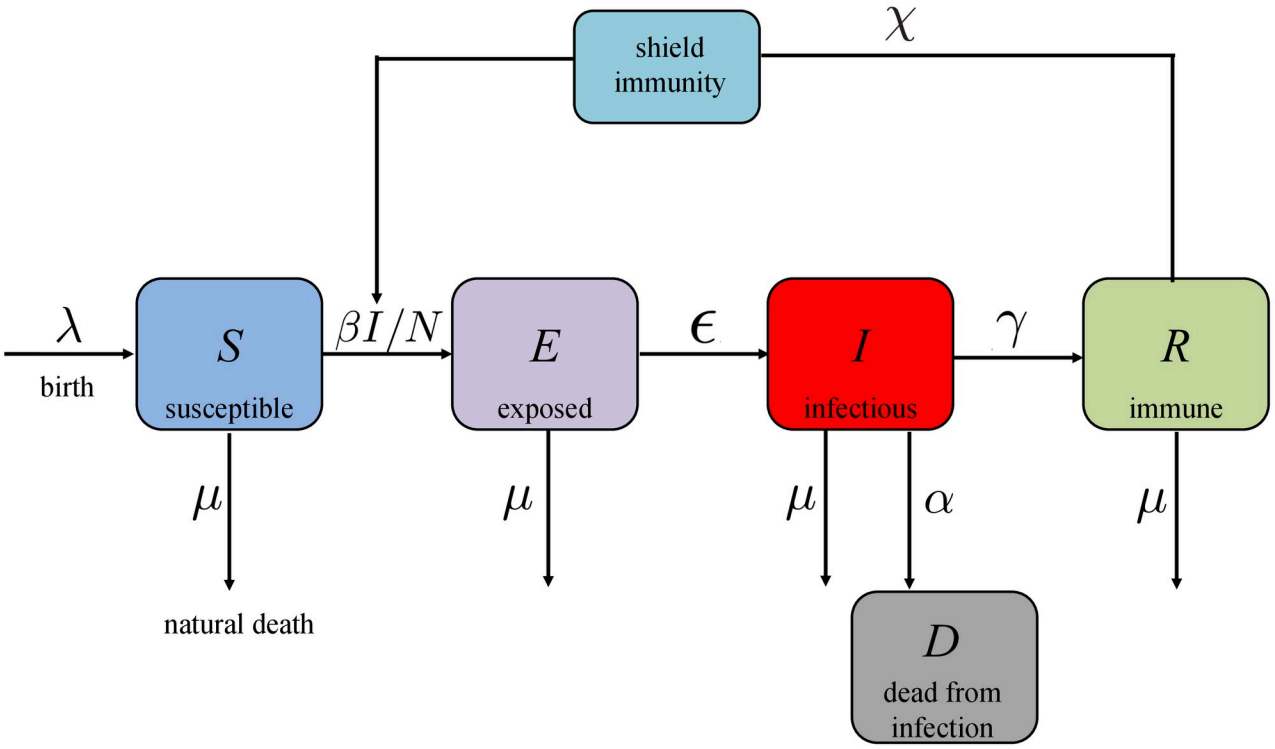

Fig 2. Block diagram of the COVID-19 SEIR model with shield immunity control.

https://doi.org/10.1371/journal.pone.0247660.g002

- The confirmed infected population C: the individuals who are confirmed to be infected with the disease (i.e., the positive cases).

We consider the SUQC model with quarantine control as follows.

$$\begin{aligned}\dot{S} &= -\beta_0 US/N;\\ \dot{U} &= \beta_0 US/N - qU;\\ \dot{Q} &= qU - (\gamma_2 + (1-\gamma_2)\sigma)Q;\\ \dot{C} &= (\gamma_2 + (1-\gamma_2)\sigma)Q,\end{aligned} \tag{5}$$

where q is the quarantine rate (for an un-quarantined infected to be quarantined) as control input to be synthesized, S, U, Q and C are the number of susceptible, un-quarantined infected, quarantined infected and confirmed infected population in the region, respectively, β_0 is the infection rate (i.e., the mean number of new infected caused by an un-quarantined infected per day), γ_2 is the confirmation rate of Q (i.e., the probability that the quarantined infected are identified to be confirmed cases through conventional methods such as laboratory diagnosis),

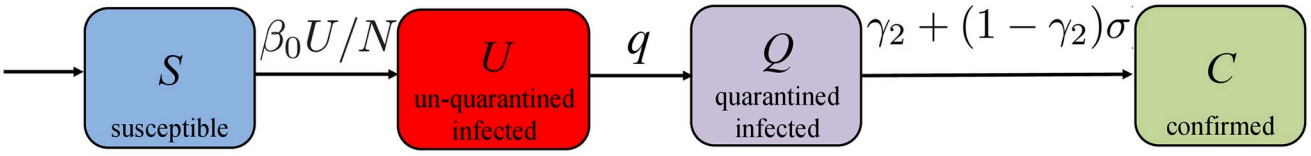

Fig 3. Block diagram of the COVID-19 SUQC model with quarantine control.

https://doi.org/10.1371/journal.pone.0247660.g003

σ is the subsequent confirmation rate of those infected that are not confirmed by the conventional methods, but confirmed with additional tests.

3.3 Control synthesis of COVID-19 epidemic with metric temporal logic specifications

In this subsection, we present the control synthesis methods for the three COVID-19 epidemic models in Section 3.2 with vaccination control, shield immunity control and quarantine control, respectively.

Vaccination control. For the COVID-19 SEIR model with vaccination control, we discretize the model in (3) as follows.

$$\begin{aligned}
I[k+1] &= I[k] + T_s\epsilon E[k] - T_s(\gamma+\mu+\alpha)I[k];\\
E[k+1] &= E[k] + T_s\beta S[k]I[k]/N[k] - T_s(\mu+\epsilon)E[k];\\
S[k+1] &= S[k] + T_s\lambda N[k] - T_s\mu S[k] - T_s\beta S[k]I[k]/N[k]\\
&\quad - T_s V[k];\\
R[k+1] &= R[k] + T_s\gamma I[k] - T_s\mu R[k] + T_s V[k];\\
D[k+1] &= D[k] + T_s\alpha I[k],
\end{aligned} \tag{6}$$

where T_s is the sampling period. We also use $\Delta D[k] = D[k] - D[k-1]$ to denote the number of deaths from the infection at day k.

Following the notations in Section 3.1, we use $x_V = [I, E, S, R, D]$ to denote the state of (6) and $\xi^V_{\cdot;x_V^{init},V}$ to denote the trajectory of (6) starting from $x_V^{init} = [I[0], E[0], S[0], R[0], D[0]]$ and vaccination control input $V[\cdot]$.

Problem 1 (Vaccination control). *Given the SEIR model with vaccination control in (6) and an MTL specification φ_V, compute the control input $V[\cdot]$ that minimizes the vaccination control efforts $\|V[\cdot]\|$ while satisfying $\langle\langle\varphi_V\rangle\rangle(\xi^V_{\cdot;x_V^{init},V}, 0) = \top$, i.e., the trajectory $\xi^V_{\cdot;x_V^{init},V}$ satisfies the MTL specification φ_V.*

The vaccination control synthesis problem can be formulated as a constrained optimization problem as follows.

$$\begin{aligned}
\min_{V[\cdot]}\quad & \|V[\cdot]\|\\
\text{s.t.}\quad & I[k+1] = I[k] + T_s\epsilon E[k] - T_s(\gamma+\mu+\alpha)I[k],\\
&\qquad \forall k = 0,\cdots,T-1,\\
& E[k+1] = E[k] + T_s\beta S[k]I[k]/N[k] - T_s(\mu+\epsilon)E[k],\\
&\qquad \forall k = 0,\cdots,T-1,\\
& S[k+1] = S[k] + T_s\lambda N[k] - T_s\mu S[k] - T_s\beta S[k]I[k]/N[k]\\
&\qquad - T_s V[k], \forall k = 0,\cdots,T-1,\\
& R[k+1] = R[k] + T_s\gamma I[k] - T_s\mu R[k] + T_s V[k],\\
&\qquad \forall k = 0,\cdots,T-1,\\
& D[k+1] = D[k] + T_s\alpha I[k], \forall k = 0,\cdots,T-1,\\
& 0 \le V[k] \le S[k], \forall k = 0,\cdots,T,\\
& \langle\langle\varphi_V\rangle\rangle(\xi^V_{\cdot;x_V^{init},V}, 0) = \top,
\end{aligned} \tag{7}$$

where $T \in \mathbb{I}$ is the maximal time index we consider.

The above optimization problem is generally a mixed-integer non-linear programming problem. We refer the readers to [38] for a detailed description of how the constraint $\langle\langle\varphi_{\mathrm{V}}\rangle\rangle(\xi^{\mathrm{V}}_{\cdot;x^{init}_{\mathrm{V}},V},0)=\top$ is encoded to satisfy an MTL specification φ_{V}. The integer variables are introduced when a *big-M formulation* [46] is needed to satisfy MTL specifications such as $\Diamond_{[0,10]}\varphi$ (φ should hold true for at least one day during the first 10 days) or $\varphi_1\vee\varphi_2$ (at least one of the MTL formulas φ_1, φ_2 should hold true). As the change of total population is relatively small compared to the multiplication of the susceptible population and the infectious population, we approximate the term $T_s\beta S[k]I[k]/N[k]$ with $T_s\beta S[k]I[k]/N_0$. With such an approximation, the optimization problem becomes a mixed-integer bi-linear programming problem, which can be more efficiently solved using techniques such as McCormick's relaxation [47, 48]. Furthermore, if the MTL specification φ consists of only conjunctions ($\wedge$) and the always operator ($\Box$), the integers in the optimization problem can be eliminated [38] and the problem becomes a bi-linear programming problem.

Shield immunity control. For the COVID-19 SEIR model with shield immunity control, we discretize the model in (4) as follows.

$$\begin{aligned}
I[k+1] &= I[k]+T_s\epsilon E[k]-T_s(\gamma+\mu+\alpha)I[k];\\
E[k+1] &= E[k]+T_s\beta S[k]I[k]/(N[k]+\chi[k]R[k])\\
&\quad -T_s(\mu+\epsilon)E[k];\\
S[k+1] &= S[k]+T_s\lambda N[k]-T_s\mu S[k]-T_s\beta S[k]I[k]/(N[k]\\
&\quad +\chi[k]R[k]);\\
R[k+1] &= R[k]+T_s\gamma I[k]-T_s\mu R[k];\\
D[k+1] &= D[k]+T_s\alpha I[k],
\end{aligned}\tag{8}$$

where T_s is the sampling period.

Following the notations in Section 3.1, we use $x_{\mathrm{S}}=[I,E,S,R,D]$ to denote the state of (8) and $\xi^{\mathrm{S}}_{\cdot;x^{init}_{\mathrm{S}},\chi}$ to denote the trajectory of (8) starting from $x^{init}_{\mathrm{S}}=[I[0],E[0],S[0],R[0],D[0]]$ and shield immunity control input $\chi[\cdot]$.

Problem 2 (Shield immunity control). *Given the SEIR model with shield immunity control in (8) and an MTL specification φ_{S}, compute the control input $\chi[\cdot]$ that minimizes the shield immunity control efforts $\|\chi[\cdot]\|$ while satisfying $\langle\langle\varphi_{\mathrm{S}}\rangle\rangle(\xi^{\mathrm{S}}_{\cdot;x^{init}_{\mathrm{S}},\chi},0)=\top$, i.e., the trajectory $\xi^{\mathrm{S}}_{\cdot;x^{init}_{\mathrm{S}},\chi}$ satisfies the MTL specification φ_{S}.*

The shield immunity control synthesis problem can be formulated as a constrained optimization problem as follows.

$$
\begin{aligned}
\min_{\chi[\cdot]} \quad & \|\chi[\cdot]\| \\
\text{s.t.} \quad & I[k+1] = I[k] + T_s \epsilon E[k] - T_s(\gamma + \mu + \alpha) I[k], \\
& \qquad \forall k = 0, \cdots, T-1, \\
& E[k+1] = E[k] + T_s \beta S[k] I[k] / (N[k] + \chi[k] R[k]) \\
& \qquad - T_s(\mu + \epsilon) E[k], \forall k = 0, \cdots, T-1, \\
& S[k+1] = S[k] + T_s \lambda N[k] - T_s \mu S[k] - T_s \beta S[k] \\
& \qquad \times I[k] / (N[k] + \chi[k] R[k]), \forall k = 0, \cdots, T-1, \\
& R[k+1] = R[k] + T_s \gamma I[k] - T_s \mu R[k], \forall k = 0, \cdots, T-1, \\
& D[k+1] = D[k] + T_s \alpha I[k], \forall k = 0, \cdots, T-1, \\
& 0 \leq \chi[k] \leq \chi_{\max}, \forall k = 0, \cdots, T, \\
& \langle\langle \varphi_S \rangle\rangle (\xi^S_{\cdot; x_S^{init}, \chi}, 0) = \top,
\end{aligned}
\tag{9}
$$

where $T \in \mathbb{I}$ is the maximal time index we consider, and $\chi_{\max}$ is the maximal shield strength.

The above optimization problem is generally a mixed-integer fractional constrained programming problem. If the MTL specification φ consists of only conjunctions ($\wedge$) and the always operator ($\Box$), the integers in the optimization problem can be eliminated [38] and the problem becomes a fractional constrained programming problem.

Quarantine control. For the COVID-19 SUQC model with quarantine control, we discretize the model in (5) as follows.

$$
\begin{aligned}
& S[k+1] = S[k] - T_s \beta_0 U[k] S[k] / N[k]; \\
& U[k+1] = U[k] + T_s \beta_0 U[k] S[k] / N[k] - q[k] U[k]; \\
& Q[k+1] = Q[k] + T_s q[k] U[k] - T_s(\gamma_2 + (1-\gamma_2)\sigma) Q[k]; \\
& C[k+1] = C[k] + T_s(\gamma_2 + (1-\gamma_2)\sigma) Q[k],
\end{aligned}
\tag{10}
$$

where T_s is the sampling period. We also use $\Delta C[k] = C[k] - C[k-1]$ to denote the number of confirmed infected individuals at day k.

Following the notations in Section 3.1, we use $x_Q = [S, U, Q, C]$ to denote the state of (10) and $\xi^Q_{\cdot; x_Q^{init}, q}$ to denote the trajectory of (10) starting from $x_Q^{init} = [S[0], U[0], Q[0], C[0]]$ and quarantine control input $q[\cdot]$.

Problem 3 (Quarantine control). *Given the SUQC model with quarantine control in*(10)*and an MTL specification* φ_Q*, compute the control input* $q[\cdot]$ *that minimizes the quarantine control efforts* $\|q[\cdot]\|$ *while satisfying* $\langle\langle \varphi_Q \rangle\rangle (\xi^Q_{\cdot; x_Q^{init}, q}, 0) = \top$*, i.e., the trajectory* $\xi^Q_{\cdot; x_Q^{init}, q}$ *satisfies the MTL specification* φ_Q.

The quarantine control synthesis problem can be formulated as a constrained optimization problem as follows.

$$\begin{aligned}
\min_{q[\cdot]} \quad & \|q[\cdot]\| \\
\text{s.t.} \quad & S[k+1] = S[k] - T_s\beta_0 U[k]S[k]/N[k], \forall k = 0, \cdots, T-1, \\
& U[k+1] = U[k] + T_s\beta_0 U[k]S[k]/N[k] - q[k]U[k], \\
& \qquad \forall k = 0, \cdots, T-1, \\
& Q[k+1] = Q[k] + T_s q[k]U[k] - T_s(\gamma_2 + (1-\gamma_2)\sigma)Q[k], \\
& \qquad \forall k = 0, \cdots, T-1, \\
& C[k+1] = C[k] + T_s(\gamma_2 + (1-\gamma_2)\sigma)Q[k], \\
& \qquad \forall k = 0, \cdots, T-1, \\
& 0 \leq q[k] \leq q_{\max}, \forall k = 0, \cdots, T, \\
& \langle\langle \varphi_Q \rangle\rangle (\xi^Q_{\cdot, x_Q^{init}, q}, 0) = \top,
\end{aligned} \tag{11}$$

where $T \in \mathbb{I}$ is the maximal time index we consider, and $q_{\max}$ is the maximal quarantine rate.

The above optimization problem is generally a mixed-integer non-linear programming problem. As the change of total population is relatively small compared to the multiplication of the susceptible population and the un-quarantined infectious population, we approximate the term $T_s\beta_0 U[k]S[k]/N[k]$ with $T_s\beta_0 U[k]S[k]/\hat{N}_0$ (we use $\hat{N}_0$ to denote the initial population in the region in the scenario with quarantine control). With such an approximation, the optimization problem becomes a mixed-integer bi-linear programming problem, which can be more efficiently solved using techniques such as McCormick's relaxation [47, 48]. Furthermore, if the MTL specification φ consists of only conjunctions ($\wedge$) and the always operator ($\Box$), the integers in the optimization problem can be eliminated [38] and the problem becomes a bi-linear programming problem.

4 Results

In this section, we implement the proposed control synthesis methods in the COVID-19 models estimated from data in Lombardy, Italy and Wuhan, China.

4.1 COVID-19 SEIR model with vaccination control

The parameters of the COVID-19 SEIR model are shown in Table 1. They were estimated using the data from February 23 to March 16, 2020 in Lombardy, Italy with no isolation

Table 1. Parameters of COVID-19 SEIR model estimated from data from Lombardy, Italy from February 23 to March 16 (2020) with no isolation measures [14].

parameter	value	parameter	value
λ	1/30295	ϵ	0.2/day
μ	1/30295	γ	0.2/day
α	0.006/day	N_0	10 million
β	0.75/day	T_s	1 day

https://doi.org/10.1371/journal.pone.0247660.t001

Table 2. MTL specifications and simulation results for vaccination control (Section 4.1).

MTL specification	control effort	computation time
$\varphi_V^1 = \square_{[0,100]}(\Delta D \leq 0.001) \wedge \square_{[0,100]}(D \leq 0.05) \wedge \Diamond_{[40,60]}(R \geq 6)$	1.28	1.365 s
$\varphi_V^2 = \square_{[0,100]}(\Delta D \leq 0.0005) \wedge \square_{[0,100]}(D \leq 0.02) \wedge \Diamond_{[40,60]}(R \geq 6)$	1.927	2.276 s
$\varphi_V^3 = \square_{[0,100]}(\Delta D \leq 0.0001) \wedge \square_{[0,100]}(D \leq 0.01) \wedge \Diamond_{[40,60]}(R \geq 6)$	6.934	3.289 s

https://doi.org/10.1371/journal.pone.0247660.t002

measures (see Section 4.1 in [14] for details). Specifically, in Table 1, the values of λ and μ are from "$\mu^{-1} \approx 83$ years" (as 83 years = 30295 days) in Section 4 in [14] and our assumption that $\lambda = \mu$, the values of α, β, ϵ and γ are from the initial values listed in Table 1 in [14], and the value of N_0 is from Lombardy's population listed in Wikipedia (https://en.wikipedia.org/wiki/Lombardy). The start time for the simulations in this subsection is February 23, 2020. We consider three MTL specifications as shown in Table 2. For example, $\varphi_V^1 = \square_{[0,100]}(\Delta D \leq 0.001) \wedge \square_{[0,100]}(D \leq 0.05) \wedge \Diamond_{[40,60]}(R \geq 6)$, which means "the deaths from COVID-19 should never exceed 0.001 million (i.e., one thousand) per day and 0.05 million (i.e., 50 thousand) in total within the next 100 days, and the immune population should eventually exceed 6 million within the next 40 to 60 days". Following Section 4.1 in [14, we choose the initial values of the states as $I[0] = 1000$ (people), $E[0] = 0.02$ million, $S[0] = 9.979$ million, $R[0] = 0$ and $D[0] = 0$, with $S[0] + E[0] + I[0] + R[0] + D[0] = N_0 = 10$ million. Fig 4 shows the simulation results without any vaccination. It can be seen that the three MTL specifications φ_V^1, φ_V^2 and φ_V^3 are all violated in such a situation. Note that as isolation measures (i.e., home isolation, social distancing and partial national lockdown) were taken since March 16 in Lombardy, Italy, the real situation was better than those shown in Fig 4. Now we investigate the hypothetical scenario where the isolation measures are replaced by vaccination.

We use the solver GEKKO [11] to solve the optimization problems formulated in Section 3.3. Fig 5 and Table 2 show the simulation results for vaccination control of COVID-19 SEIR model with MTL specifications φ_V^1, φ_V^2 and φ_V^3, respectively. The results show that the MTL specifications φ_V^1, φ_V^2 and φ_V^3 are satisfied with the synthesized vaccination control inputs respectively. It can be seen that vaccination within the first 40 days after the outbreak can mitigate the spread of SARS-CoV-2 in the most efficient manner. The results also show that the control effort for satisfying φ_V^1 is less than that for satisfying φ_V^2, which is still less than that for satisfying φ_V^3. This is consistent with the fact that φ_V^2 implies φ_V^1, and φ_V^3 implies both φ_V^1 and φ_V^2. For all three specifications, the computations are completed within 4 seconds on a MacBook laptop with 1.40-GHz Core i5 CPU and 16-GB RAM.

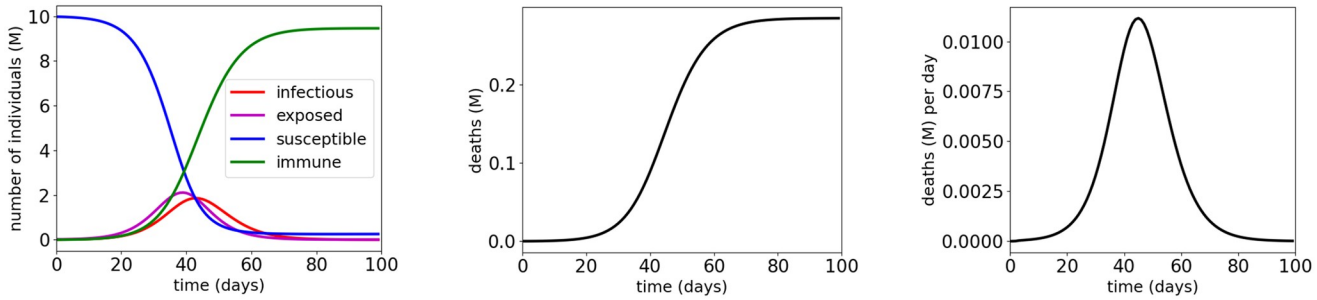

Fig 4. Simulation results for COVID-19 SEIR model estimated from data from Lombardy, Italy with no isolation measures.

https://doi.org/10.1371/journal.pone.0247660.g004

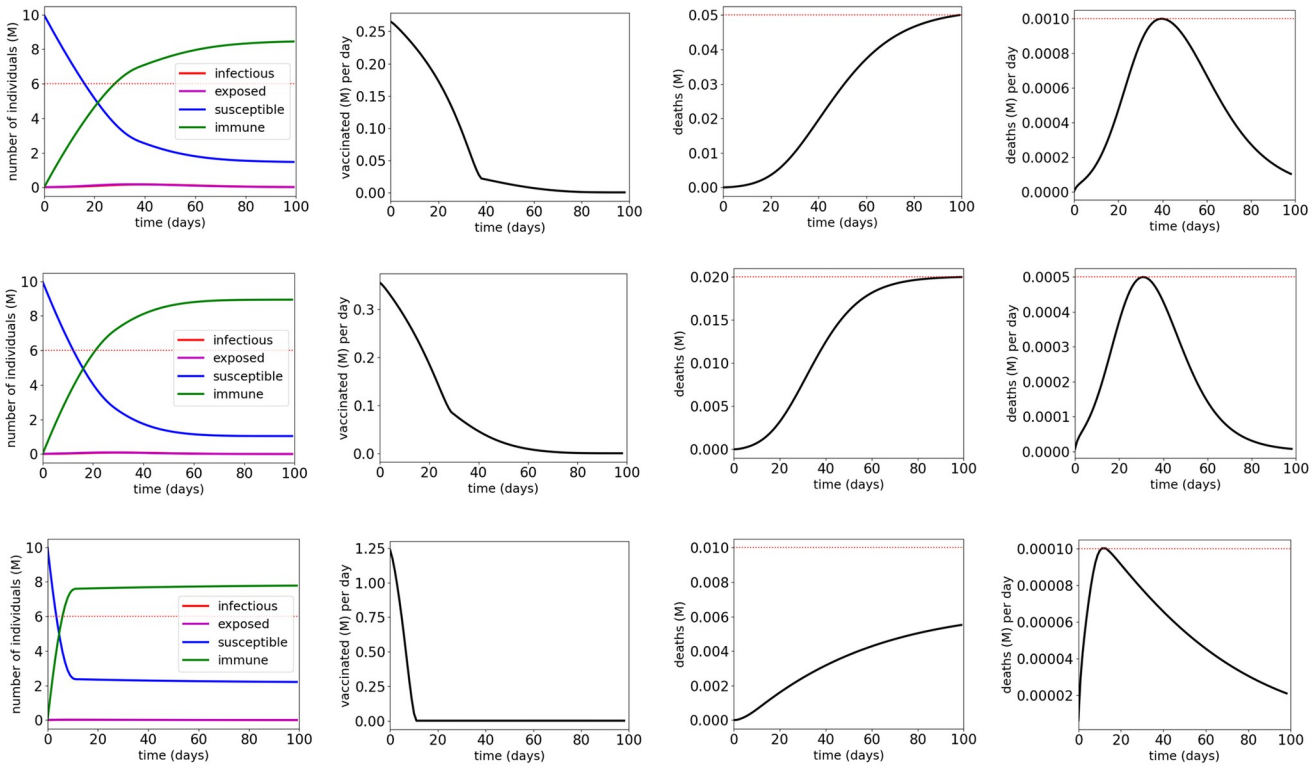

Fig 5. Simulation results for the COVID-19 SEIR model with vaccination control and MTL specifications φ_V^1 (first row), φ_V^2 (second row) and φ_V^3 (third row). The red dotted lines indicate the thresholds in the atomic propositions of the MTL specifications φ_V^1, φ_V^2 and φ_V^3.

https://doi.org/10.1371/journal.pone.0247660.g005

4.2 COVID-19 SEIR model with shield immunity control

We use the same parameters of the COVID-19 SEIR model as shown in Table 1 (in the same setting as in Section 4.1 for Lombardy, Italy, with no isolation measures). Following Section 4.1 in [14], we choose the initial values of the states as $I[0] = 1000$ (people), $E[0] = 0.02$ million, $S[0] = 9.979$ million, $R[0] = 0$ and $D[0] = 0$, with $S[0] + E[0] + I[0] + R[0] + D[0] = N_0 = 10$ million. We set $\chi_{\max} = 100$. The start time for the simulations in this subsection is February 23, 2020. We set the three MTL specifications φ_S^1, φ_S^2 and φ_S^3 (as shown in Table 3) to be less stringent than the MTL specifications with the vaccination control, as shield immunity is generally less effective than vaccination. It can be shown that without any control strategies the three MTL specifications φ_S^1, φ_S^2 and φ_S^3 are all violated. Now we investigate the hypothetical scenario where the isolation measures are replaced by shield immunity control.

Fig 6 and Table 3 show the simulation results for shield immunity control of the COVID-19 SEIR model with MTL specifications φ_S^1, φ_S^2 and φ_S^3, respectively. The results show that the

Table 3. MTL specifications and simulation results for shield immunity control (Section 4.2).

MTL specification	control effort	computation time
$\varphi_S^1 = \Box_{[0,100]}(\Delta D \leq 0.003) \wedge \Box_{[0,100]}(D \leq 0.01) \wedge \Diamond_{[40,60]}(R \geq 1)$	16879.53	2.112 s
$\varphi_S^2 = \Box_{[0,100]}(\Delta D \leq 0.002) \wedge \Box_{[0,100]}(D \leq 0.07) \wedge \Diamond_{[40,60]}(R \geq 1)$	45595.10	2.881 s
$\varphi_S^3 = \Box_{[0,100]}(\Delta D \leq 0.002) \wedge \Box_{[0,100]}(D \leq 0.06) \wedge \Diamond_{[40,60]}(R \geq 1)$	67786.88	5.323 s

https://doi.org/10.1371/journal.pone.0247660.t003

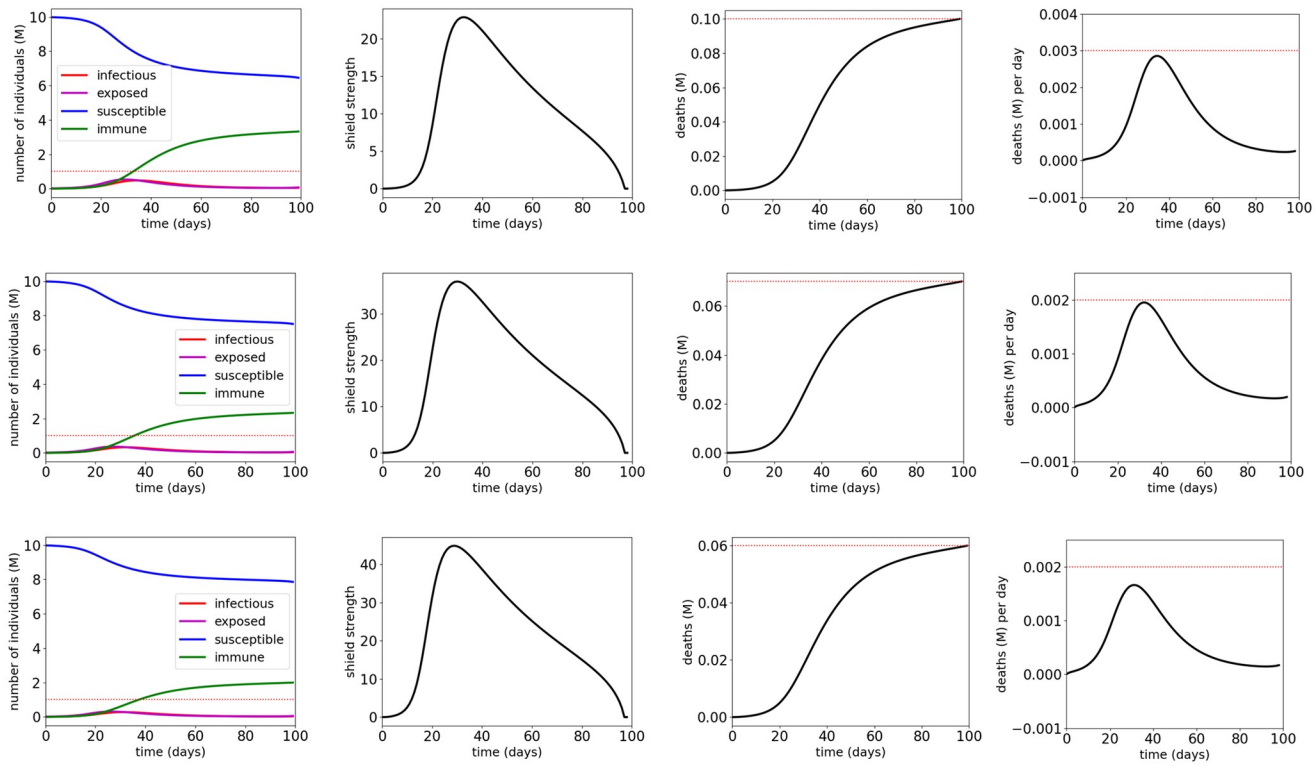

Fig 6. Simulation results for the COVID-19 SEIR model with shield immunity control and MTL specifications φ_S^1 (first row), φ_S^2 (second row) and φ_S^3 (third row). The red dotted lines indicate the thresholds in the atomic propositions of the MTL specifications φ_S^1, φ_S^2 and φ_S^3.

https://doi.org/10.1371/journal.pone.0247660.g006

MTL specifications φ_S^1, φ_S^2 and φ_S^3 are satisfied with the synthesized shield immunity control inputs respectively. We observe that with the three MTL specifications, the synthesized shield immunity control inputs all increase to a peak after approximately 20 to 40 days and then gradually decrease. These observations indicate that shield immunity at early days of COVID-19 is more efficient than shield immunity at later days. The results also show that the control effort for satisfying φ_S^1 is less than that for satisfying φ_S^2, which is still less than that for satisfying φ_S^3. This is consistent with the fact that φ_S^2 implies φ_S^1, and φ_S^3 implies both φ_S^1 and φ_S^2.

4.3 COVID-19 SUQC model with quarantine control

The parameters of the COVID-19 SUQC model are shown in Table 4. In Table 4, the value of the infection rate β_0 is from "Methods/Parameter inference" in [7] (the authors in [7] used α to denote the infection rate), the value of $\hat{N}_0$ is from Wuhan's urban population listed in Wikipedia (https://en.wikipedia.org/wiki/Wuhan), the value of the confirmation rate γ_2 is from the confirmation rate listed under Stage I (January 20 to January 30, 2020) of Wuhan in Table 1

Table 4. Parameters of the COVID-19 SUQC model estimated from data in Stage I (January 20 to January 30, 2020) of Wuhan, China [7].

parameter	value	parameter	value
β_0	0.2967	γ_2	0.05
$\hat{N}_0$	8.9 million	σ	0
T_s	1 day		

https://doi.org/10.1371/journal.pone.0247660.t004

Table 5. MTL specifications and simulation results for quarantine control (Section 4.3).

MTL specification	control effort	computation time
$\varphi_{\mathrm{Q}}^{1} = \square_{[0,200]}(\Delta C \leq 0.001) \wedge \square_{[0,200]}(C \leq 0.01)$	15.146	2.296 s
$\varphi_{\mathrm{Q}}^{2} = \square_{[0,200]}(\Delta C \leq 0.0005) \wedge \square_{[0,200]}(C \leq 0.05)$	15.638	2.598 s
$\varphi_{\mathrm{Q}}^{3} = \square_{[0,200]}(\Delta C \leq 0.0005) \wedge \square_{[0,200]}(C \leq 0.03)$	15.894	4.578 s

https://doi.org/10.1371/journal.pone.0247660.t005

in [7], and the value of σ is from "Methods/SUQC model" in [7] when no other special approaches are used for additional tests. We choose the initial values of the states as $S[0] = 8.9$ million, $U[0] = 0.001$ million, $Q[0] = 0$ and $C[0] = 0$. We set $q_{\max} = 1$. We consider three MTL specifications as shown in Table 5. For example, $\varphi_{\mathrm{Q}}^{1} = \square_{[0,200]}(\Delta C \leq 0.001) \wedge \square_{[0,200]}(C \leq 0.1)$ means "the confirmed infected population should never exceed 0.001 million (i.e., one thousand) per day and 0.1 million (i.e., 100 thousand) in total within the next 200 days". The start time for the simulations in this subsection is January 20, 2020. Fig 7 shows the simulation results for the COVID-19 SUQC model with parameters in Table 4 (estimated from data in Stage I of Wuhan, China). It can be seen that the three MTL specifications φ_{Q}^{1}, φ_{Q}^{2} and φ_{Q}^{3} are all violated in such a situation (with quarantine rate being always 0.063). Now we investigate the scenario where the quarantine rate can be controlled to satisfy the MTL specifications.

Fig 8 and Table 5 show the simulation results for quarantine control of the COVID-19 SUQC model with MTL specifications φ_{Q}^{1}, φ_{Q}^{2} and φ_{Q}^{3}, respectively. The results show that the MTL specifications φ_{Q}^{1}, φ_{Q}^{2} and φ_{Q}^{3} are satisfied with the synthesized quarantine control inputs respectively. The results also show that the control effort for satisfying φ_{Q}^{1} is less than that for satisfying φ_{Q}^{2}, which is still less than that for satisfying φ_{Q}^{3}. This is consistent with the fact that φ_{Q}^{2} implies φ_{Q}^{1}, and φ_{Q}^{3} implies both φ_{Q}^{1} and φ_{Q}^{2}. We observe that with φ_{Q}^{1}, the synthesized quarantine control inputs first increase to a peak at approximately 90 days and then gradually decrease for most of the time; with φ_{Q}^{2}, the synthesized quarantine control inputs first increase to a peak at approximately 50 days and then gradually decrease for most of the time; and with φ_{Q}^{3}, the synthesized quarantine control inputs are at a peak from the beginning and gradually decrease for most of the time. These observations indicate that quarantine in the early days of COVID-19 can reduce the number of confirmed infected cases more efficiently than quarantine in the later days, and more stringent control specifications require stronger quarantine measures to be implemented.

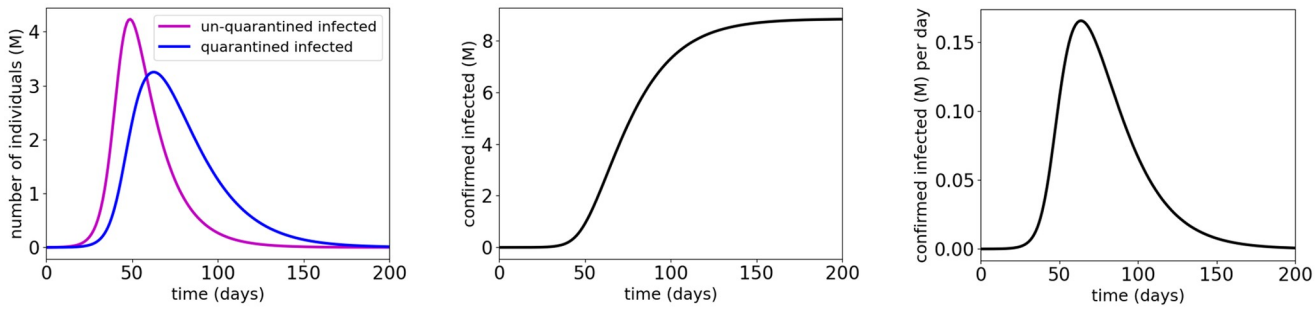

Fig 7. Simulation results for the COVID-19 SUQC model estimated from data in Stage I of Wuhan, China.

https://doi.org/10.1371/journal.pone.0247660.g007

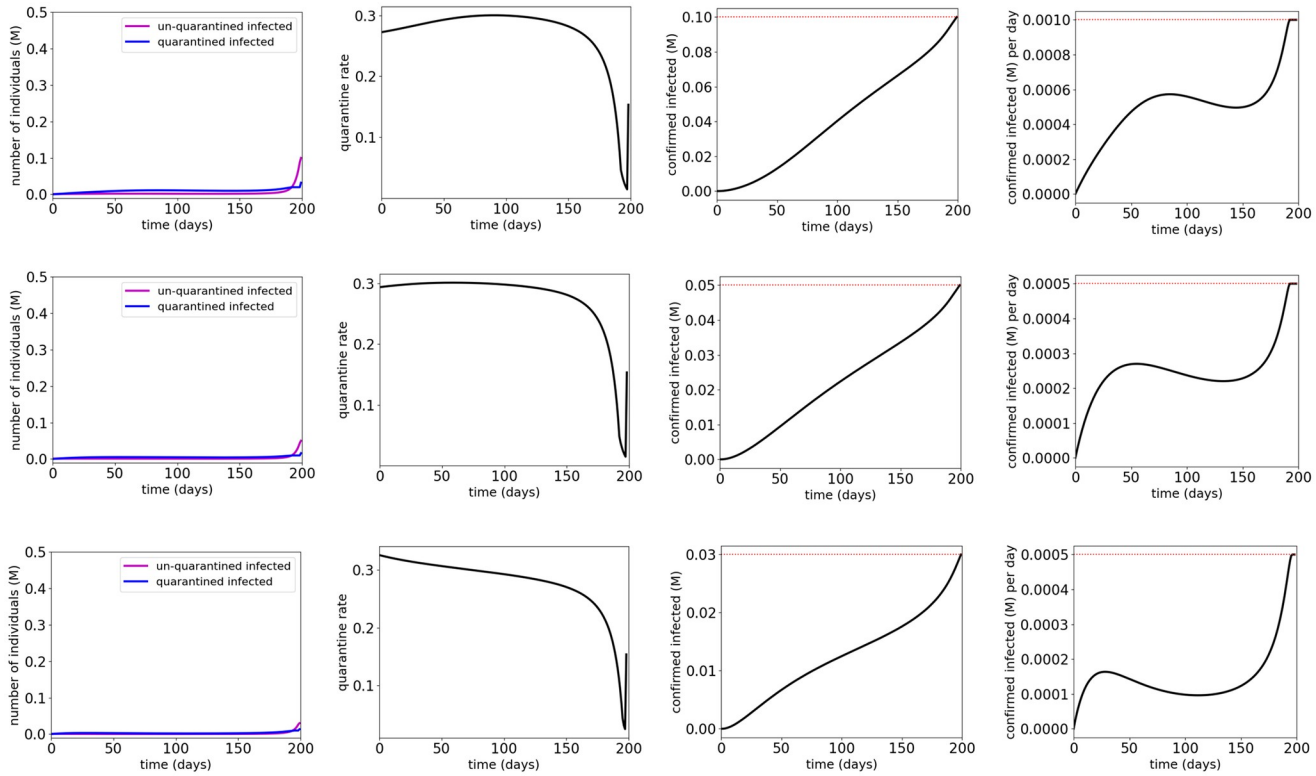

Fig 8. Simulation results for the COVID-19 SUQC model with quarantine control and MTL specifications φ_Q^1 (first row), φ_Q^2 (second row) and φ_Q^3 (third row). The red dotted lines indicate the thresholds in the atomic propositions of the MTL specifications φ_Q^1, φ_Q^2 and φ_Q^3.

https://doi.org/10.1371/journal.pone.0247660.g008

5 Discussion

In this paper, we proposed a systematic control synthesis approach for mitigating the COVID-19 epidemic based on three control models with vaccination, shield immunity and quarantine, respectively. We used metric temporal logic (MTL) formulas to formally specify the required performance of the control strategies. The proposed approach can synthesize control inputs that lead to satisfaction of the MTL specifications. The methodology and results in this paper contribute to several useful suggestions on limiting the spread of COVID-19.

Firstly, from the results with three control strategies (vaccination, shield immunity and quarantine) we observe the unanimous trend that the computed optimal control values are larger in the earlier days after the outbreak. This indicates that early intervention is essential and the most efficient (in comparison with late intervention) in controlling the spread of COVID-19.

Secondly, while it is obvious that more control efforts are needed to achieve more stringent control specifications, we observe that the required control efforts are not linear with respect to the "stringency" of the control specifications. For example, based on the model in Lombardy, Italy, achieving less than 20000 total deaths and 500 deaths per day within 100 days requires 50.55% more vaccination control effort than achieving less than 50000 total deaths and 1000 deaths per day within 100 days. However, achieving less than 10000 total deaths and 100 deaths per day within 100 days requires 259.83% more vaccination control effort than achieving less than 20000 total deaths and 500 deaths per day within 100 days. This "diminishing return" kind of property indicates that the same amount of additional (vaccination)

control efforts will generally achieve less improvement for the control performance when the control specifications are increasingly more stringent.

The work in this paper opens the door to the formal synthesis of control strategies based on epidemic models. We believe that the methodology we developed in this paper can be readily used in controlling COVID-19 (and potentially other epidemic diseases) in various places where the control outcome needs to be specified in precise manners. In the following, we list several future directions that may readily derive from the work in this paper.

Firstly, the validity of the results depends on the accuracy of the model parameters (e.g., the recovery rate γ of infectious individuals). However, as the computation time is relatively short (within 6 seconds for all the scenarios in this paper), the user (or decision maker) can always change the model parameters to the latest estimated parameters and compute the optimal controls in a short time. The work in this paper can be readily extended to online control synthesis so that control inputs can be generated in real-time based on the latest information (e.g., using online parameter identification and receding horizon control).

Secondly, as we investigated the three control strategies separately in this paper, we will study the benefits and costs of joint control of different control strategies (vaccination, shield immunity and quarantine) so that the specifications can be satisfied with coordinated efforts. For example, to study the coordinated control of vaccination and shield immunity, we can use an integrated SEIR model with both V and $N + \chi R$. By selecting a cost function being the weighted sum of $\|V[\cdot]\|$ and $\|\chi[\cdot]$, we can achieve coordinated control of vaccination and shield immunity where the weights for $\|V[\cdot]\|$ and $\|\chi[\cdot]$ represent the relative costs of vaccination and shield immunity. To further include quarantine control, we can resort to more detailed models that differentiate between quarantined and un-quarantined population (e.g., as described in [49]).

Thirdly, the results in this paper focus on the control of COVID-19 in one specific region (i.e., Lombardy, Italy and Wuhan, China). Due to different geographic and demographic characteristics, the parameters in the COVID-19 models in different regions may be different, and the specifications in different regions may also be different (more stringent specifications for regions where the policy focuses more on mitigating the spread of COVID-19 than other factors such as the impact on the economy). The methodology in this paper can be readily applied to synthesizing coordinated regional control strategies for multiple different yet somewhat connected regions (e.g., as described in [49]).

Author Contributions

Conceptualization: Zhe Xu, Bo Wu.

Data curation: Zhe Xu.

Formal analysis: Zhe Xu.

Investigation: Zhe Xu.

Methodology: Zhe Xu, Bo Wu.

Project administration: Ufuk Topcu.

Resources: Zhe Xu.

Software: Zhe Xu.

Supervision: Ufuk Topcu.

Validation: Zhe Xu.

Visualization: Zhe Xu.

Writing – original draft: Zhe Xu.

Writing – review & editing: Zhe Xu, Bo Wu, Ufuk Topcu.

References

1. Fauci AS, Lane HC, Redfield RR. COVID-19—Navigating the Uncharted. New England Journal of Medicine. 2020; 382(13):1268–1269. https://doi.org/10.1056/NEJMe2002387
2. Stewart G, Heusden K, Dumont GA. How control theory can help us control COVID-19. IEEE Spectrum. 2020; 57(6):22–29. https://doi.org/10.1109/MSPEC.2020.9099929
3. Yang P, Qi J, Zhang S, Wang X, Bi G, Yang Y, et al. Feasibility study of mitigation and suppression strategies for controlling COVID-19 outbreaks in London and Wuhan. PLOS ONE. 2020; 15(8):1–19. https://doi.org/10.1371/journal.pone.0236857 PMID: 32760081
4. Zhang L, Tao Y, Shen M, Fairley CK, Guo Y. Can self-imposed prevention measures mitigate the COVID-19 epidemic? PLOS Medicine. 2020; 17(7):1–4.
5. Callaway E. The race for coronavirus vaccines: a graphical guide. Nature. 2020; 580:576–577. https://doi.org/10.1038/d41586-020-01221-y
6. Weitz J, Beckett S, Coenen A, David D, Dominguez-Mirazo M, Dushoff J, et al. Intervention Serology and Interaction Substitution: Modeling the Role of 'Shield Immunity' in Reducing COVID-19 Epidemic Spread. Nature Medicine. 2020; p. 849–854.
7. Zhao S, Chen H. Modeling the epidemic dynamics and control of COVID-19 outbreak in China. Quantitative biology (Beijing, China). 2020; p. 1–9.
8. Xu Z, Topcu U. Transfer of Temporal Logic Formulas in Reinforcement Learning. In: Proc. IJCAI'2019; 2019. p. 4010–4018.
9. Verginis CK, Vrohidis C, Bechlioulis CP, Kyriakopoulos KJ, Dimarogonas DV. Reconfigurable Motion Planning and Control in Obstacle Cluttered Environments under Timed Temporal Tasks. In: 2019 International Conference on Robotics and Automation (ICRA); 2019. p. 951–957.
10. Xu Z, Julius A, Chow JH. Energy Storage Controller Synthesis for Power Systems With Temporal Logic Specifications. IEEE Systems Journal. Early access on IEEE Xplore;.
11. Beal L, Hill D, Martin R, Hedengren J. GEKKO Optimization Suite. Processes. 2018; 6(8):106. https://doi.org/10.3390/pr6080106
12. Bertozzi AL, Franco E, Mohler G, Short MB, Sledge D. The challenges of modeling and forecasting the spread of COVID-19. Proceedings of the National Academy of Sciences. 2020; 117(29):16732–16738. https://doi.org/10.1073/pnas.2006520117
13. Chen Z, Dassios A, Kuan V, Lim JW, Qu Y, Surya B, et al. A two-phase dynamic contagion model for COVID-19. London School of Economics and Political Science, LSE Library; 2020. 105064.
14. Carcione JM, Santos JE, Bagaini C, Ba J. A Simulation of a COVID-19 Epidemic Based on a Deterministic SEIR Model. Frontiers in Public Health. 2020; 8:230. https://doi.org/10.3389/fpubh.2020.00230
15. Elie R, Hubert E, Turinici G. Contact rate epidemic control of COVID-19: an equilibrium view. 2020;.
16. Ediriweera DS, de Silva NR, Malavige GN, de Silva HJ. An epidemiological model to aid decision-making for COVID-19 control in Sri Lanka. PLOS ONE. 2020; 15(8):1–10.
17. Liu F, Wang J, Liu J, Li Y, Liu D, Tong J, et al. Predicting and analyzing the COVID-19 epidemic in China: Based on SEIRD, LSTM and GWR models. PLOS ONE. 2020; 15(8):1–22. https://doi.org/10.1371/journal.pone.0238280 PMID: 32853285
18. Zheng N, Du S, Wang J, Zhang H, Cui W, Kang Z, et al. Predicting COVID-19 in China Using Hybrid AI Model. IEEE Transactions on Cybernetics. 2020; 50(7):2891–2904. https://doi.org/10.1109/TCYB.2020.2990162 PMID: 32396126
19. Alonso-Quesada S, De la Sen M, Agarwal R, Ibeas A. An observer-based vaccination control law for a SEIR epidemic model based on feedback linearization techniques for nonlinear systems. Advances in Difference Equations. 2012; 2012.
20. de Pinho MdR, Kornienko I, Maurer H. Optimal Control of a SEIR Model with Mixed Constraints and L1 Cost. In: Moreira AP, Matos A, Veiga G, editors. CONTROLO'2014 – Proceedings of the 11th Portuguese Conference on Automatic Control. Cham: Springer International Publishing; 2015. p. 135–145.
21. Kress-Gazit H, Fainekos GE, Pappas GJ. Temporal-Logic-Based Reactive Mission and Motion Planning. Robotics, IEEE Trans. 2009; 25(6):1370–1381. https://doi.org/10.1109/TRO.2009.2030225

22. Raman V, Finucane C, Kress-Gazit H. Temporal logic robot mission planning for slow and fast actions. In: Intelligent Robots and Systems (IROS), 2012 IEEE/RSJ International Conference on; 2012. p. 251–256.

23. Lin KH, Lam KM, Siu WC. A new approach using modified Hausdorff distances with eigenface for human face recognition. In: Control, Automation, Robotics and Vision, 2002. ICARCV 2002. 7th International Conference on. vol. 2; 2002. p. 980–984 vol.2.

24. Hibbard M, Savas Y, Xu Z, Julius AA, Topcu U. Minimizing the Information Leakage of High-Level Task Specifications. In: 21st IFAC World Congress; 2020.

25. Smith SL, Tumova J, Belta C, Rus D. Optimal path planning under temporal logic constraints. In: Intelligent Robots and Systems (IROS), 2010 IEEE/RSJ Int. Conf.; 2010. p. 3288–3293.

26. Ulusoy A, Smith SL, Ding XC, Belta C, Rus D. Optimal multi-robot path planning with temporal logic constraints. In: Intelligent Robots and Systems (IROS), 2011 IEEE/RSJ Int. Conf.; 2011. p. 3087–3092.

27. Liu Z, Wu B, Dai J, Lin H. Distributed communication-aware motion planning for multi-agent systems from STL and spatel specifications. In: 2017 IEEE 56th Annual Conference on Decision and Control (CDC). IEEE; 2017. p. 4452–4457.

28. Djeumou F, Xu Z, Topcu U. Probabilistic Swarm Guidance with Graph Temporal Logic Specifications. In: Proc. Robotics: Science and Systems (RSS); 2020.

29. Liu Z, Dai J, Wu B, Lin H. Communication-aware motion planning for multi-agent systems from signal temporal logic specifications. In: 2017 American Control Conference (ACC). IEEE; 2017. p. 2516–2521.

30. Liu Z, Wu B, Dai J, Lin H. Distributed Communication-aware Motion Planning for Networked Mobile Robots under Formal Specifications. IEEE Transactions on Control of Network Systems. 2020;.

31. Cubuktepe M, Xu Z, Topcu U. Policy Synthesis for Factored MDPs with Graph Temporal Logic Specifications. In: Proc. International Conference on Autonomous Agents and Multiagent Systems (AAMAS); 2020.

32. Wolff EM, Topcu U, Murray RM. Automaton-guided controller synthesis for nonlinear systems with temporal logic. In: Proc. IEEE/RSJ Int. Conf. Intell. Robots and Syst.; 2013. p. 4332–4339.

33. Nikou A, Tumova J, Dimarogonas DV. Cooperative Task Planning of Multi-Agent Systems Under Timed Temporal Specifications. CoRR. 2015;abs/1509.09137.

34. Coogan S, Gol EA, Arcak M, Belta C. Traffic Network Control From Temporal Logic Specifications. IEEE Transa Control of Network Systems. 2016; 3(2):162–172. https://doi.org/10.1109/TCNS.2015.2428471

35. Donze A, Raman V. BluSTL: Controller Synthesis from Signal Temporal Logic Specifications. In: Frehse G, Althoff M, editors. ARCH14-15. 1st and 2nd International Workshop on Applied veRification for Continuous and Hybrid Systems. vol. 34 of EPiC Series in Computing. EasyChair; 2015. p. 160–168.

36. Xu Z, Zegers FM, Wu B, Dixon W, Topcu U. Controller Synthesis for Multi-Agent Systems With Intermittent Communication. A Metric Temporal Logic Approach. In: Allerton'19;. p. 1015–1022.

37. Xu Z, Yazdani K, Hale MT, Topcu U. Differentially Private Controller Synthesis With Metric Temporal Logic Specifications. In: To appear in Proc. International Conference on Autonomous Agents and Multiagent Systems (AAMAS); 2020.

38. Saha S, Julius AA. An MILP approach for real-time optimal controller synthesis with Metric Temporal Logic specifications. In: Proc. IEEE Amer. Control Conf.; 2016. p. 1105–1110.

39. Xu Z, Saha S, Hu B, Mishra S, Julius AA. Advisory Temporal Logic Inference and Controller Design for Semiautonomous Robots. IEEE Trans Autom Sci Eng. 2018; p. 1–19.

40. Xu Z, Julius AA, Chow JH. Coordinated Control of Wind Turbine Generator and Energy Storage System for Frequency Regulation under Temporal Logic Specifications. In: Proc. Amer. Control Conf.; 2018. p. 1580–1585.

41. Winn AK, Julius AA. Optimization of human generated trajectories for safety controller synthesis. In: Proc. IEEE Amer. Control Conf.; 2013. p. 4374–4379.

42. Abbas H, Winn A, Fainekos G, Julius AA. Functional gradient descent method for Metric Temporal Logic specifications. In: Proc. IEEE Amer. Control Conf.; 2014. p. 2312–2317.

43. Xu Z, Julius A, Chow JH. Optimal energy storage control for frequency regulation under temporal logic specifications. In: 2017 American Control Conference (ACC); 2017. p. 1874–1879.

44. Fainekos GE, Pappas GJ. Robustness of temporal logic specifications. In: Formal Approaches to Testing and Runtime Verification, in: LNCS, vol. 4262, Springer, 2006;.

45. Fainekos GE, Pappas GJ. Robustness of temporal logic specifications for continuous-time signals. Theoretical Computer Science. 2009; 410(42):4262–4291. https://doi.org/10.1016/j.tcs.2009.06.021

46. Schrijver A. Theory of Linear and Integer Programming. John Wiley & Sons, Chichester; 1986.

47. McCormick GP. Computability of global solutions to factorable nonconvex programs: Part I—Convex underestimating problems. Mathematical Programming. 1976;. https://doi.org/10.1007/BF01580665

48. Gupte A, Ahmed S, Cheon MS, Dey SS. Solving Mixed Integer Bilinear Problems Using MILP Formulations. SIAM J Optim. 2013; 23:721–744. https://doi.org/10.1137/110836183

49. Rossa FD, Salzano D, Meglio AD, Lellis FD, Coraggio M, Calabrese C, et al. Intermittent yet coordinated regional strategies can alleviate the COVID-19 epidemic: a network model of the Italian case. Nature Communications. 2020; 11 (5106).